Cortical Atrophy Predicts Visual Performance in Long-Term Central Retinal Disease; GCL, pRNFL and Cortical Thickness Are Key Biomarkers

Rachel L. W. Hanson,[1–4] Heidi A. Baseler,[1–3,5] Archana Airody,[4] Antony B. Morland,[1–3] and Richard P. Gale[4,5]

[1]Department of Psychology, University of York, York, United Kingdom
[2]York Neuroimaging Centre, University of York, York, United Kingdom
[3]York Biomedical Research Institute, University of York, York, United Kingdom
[4]Academic Unit of Ophthalmology, York and Scarborough Teaching Hospitals NHS Foundation Trust, York, United Kingdom
[5]Hull York Medical School, University of York, York, United Kingdom

Correspondence: Rachel L.W. Hanson, York and Scarborough Teaching Hospitals NHS Foundation Trust, Wigginton Road, York YO10 8HE, UK;
rachel.hanson11@nhs.net.

Received: October 28, 2021
Accepted: May 1, 2022
Published: May 27, 2022

Citation: Hanson RLW, Baseler HA, Airody A, Morland AB, Gale RP. Cortical atrophy predicts visual performance in long-term central retinal disease; GCL, pRNFL and cortical thickness are key biomarkers. *Invest Ophthalmol Vis Sci.* 2022;63(5):35.
https://doi.org/10.1167/iovs.63.5.35

Purpose. The aim of this study was to assess both retinal and cortical structure in a cohort of patients with long-term acquired central retinal disease in order to identify potential disease biomarkers and to explore the relationship between the anterior and posterior visual pathways.

Methods. Fourteen participants diagnosed with long-term central retinal disease underwent structural assessments of the retina using spectral-domain optical coherence tomography, including macular ganglion cell layer (GCL) and peripapillary retinal nerve fiber layer (pRNFL) thickness. Structural magnetic resonance imaging was used to measure visual cortex, including cortical volume of the entire occipital lobe and cortical thickness of the occipital pole and calcarine sulcus, representing the central and peripheral retina, respectively.

Results. Mean thickness was significantly reduced in both the macular GCL and the inferior temporal pRNFL across patients. Cortical thickness was significantly reduced in both the occipital pole and calcarine sulcus, representing the central and peripheral retina, respectively. Disease duration significantly correlated with GCL thickness with a large effect size, whereas a medium effect size suggests the possibility that cortical thickness in the occipital pole may correlate with visual acuity.

Conclusions. Long-term central retinal disease is associated with significant structural changes to both the retina and the brain. Exploratory analysis suggests that monitoring GCL thickness may be a sensitive biomarker of disease progression and reductions in visual cortical thickness may be associated with reduced visual acuity. Although this study is limited by its heterogeneous population, larger cohort studies would be needed to better establish some of the relationships detected between disease dependent structural properties of the anterior and posterior visual pathway given the effect sizes reported in our exploratory analysis.

Keywords: neovascular age-related macular degeneration, ganglion cell layer, peripapillary retinal nerve fiber layer, occipital cortex, cortical atrophy, vision loss

The prevalence of vision loss due to retinal disease is increasing; consequently, current research is focusing on treatment techniques to prevent disease progression in the eye and to restore visual input. However, vision restoration cannot be successful unless all parts of the visual pathways are functioning properly. Therefore, it is important to ensure that we fully understand the relationship between changes occurring in the anterior (eye) and posterior (brain) visual pathways to help determine biomarkers of disease progression, avenues for possible neuroprotection, and future restorative treatment.

Assessing changes to the anterior visual pathway resulting from retinal disease is a vital part of routine care, and spectral-domain optical coherence tomography (SD-OCT) is the tool often used to quantify changes in the thickness of many retinal structures. In neovascular age-related macular degeneration (nvAMD), a predominantly central retinal disease, SD-OCT measures the magnitude of the resulting macular edema via changes in retinal thickness, with reports indicating that reduced thickness coincides with reduced edema size following anti-vascular endothelial growth factor (anti-VEGF) treatment.[1–3] However, in nvAMD, assessing changes to specific retinal layers as opposed to total retinal thickness may be more diagnostic in the long term, as the inner retina will be less affected by subretinal fluid associated with the disease but may experience neural changes.

Investigative Ophthalmology & Visual Science

For example, some studies have reported thinning of the ganglion cell layer (GCL) in nvAMD compared with sighted controls, suggesting possible ganglion cell loss.[4–6]

SD-OCT is also used to measure changes in peripapillary retinal nerve fiber layer (pRNFL) thickness of the optic nerve head. It has been established from trajectories of the retinal nerve fiber bundles from the optic nerve head that foveal fibers occupy a large portion of the temporal quadrant.[7,8] Supporting this, significant reductions in pRNFL thickness have been reported in superior, inferior, and temporal quadrants in both nvAMD[5] and dry AMD,[9] which the authors suggest may reflect adverse reactions to repeated anti-VEGF injections and inner retinal damage, respectively.

Quantifying changes to the posterior visual pathway associated with retinal disease is most commonly assessed using magnetic resonance imaging (MRI). Significant atrophy (shrinkage) of the visual cortex has been described in AMD patients, with reductions in volume of the entire occipital lobe and significant reductions in cortical thickness in cortical representations of the affected central retina, the occipital pole.[1,10–14]

Despite our current understanding of the impact retinal disease has on the anterior and posterior visual pathways, we do not know how changes to these pathways may be related. In order for preservative and restorative treatments to be effective, we need to understand how changes to one pathway may influence the other. For example, it is important to determine whether there is evidence of retrograde and/or anterograde transsynaptic degeneration or retinal remodeling, all of which will influence how patients are treated. To address this, the current study investigated which changes occur to the anterior and posterior visual pathways, potentially identifying biomarkers of disease progression in long-term central retinal disease. The second element of this study was to conduct an exploratory analysis of possible relationships between changes in the anterior and posterior visual pathway in the same cohort, attempting to address whether such changes may reflect retrograde or anterograde degeneration, retinal remodeling, or adverse anti-VEGF response.

Materials and Methods

Participants

Written informed consent was obtained from all participants enrolled in the SYNAPTIC study. Ethical approval was granted by the York Neuroimaging Centre Research Ethics and Governance Committee and the National Health Service Research Ethics Committee (IRAS: 181823). This study followed the tenets of the Declaration of Helsinki.

Eighteen participants were recruited from York Teaching Hospital NHS Foundation Trust between November 2018 and September 2019. Inclusion criteria were bilateral vision loss due to AMD with an overlapping central scotoma, resulting in central vision loss. Exclusion criteria included any other central retinal disease, all peripheral-affecting retinal disease, contraindications for completing MRI procedures or receiving pupil dilation, enrollment in an interventional clinical trial, or inability to comply with the study. Three participants withdrew from the study before data collection; a fourth participant was unable to complete the MRI assessments and was excluded. This resulted in a final cohort of 14 participants (mean age, 78.07 years; age range, 63.07–90.10 years; six females) (Table 1). Disease duration for all partic-

Table 1. Demographics of Participants Recruited to the SYNAPTIC Study Diagnosed With Central Retinal Disease

				Worse Eye				Better Eye				
Subject	Gender	Age (y, mo)	Bilateral Diagnosis	OD/OS	BCVA	Anti-VEGF Injections, *n*	Retinal Lesion Size (mm^2)	OD/OS	BCVA	Anti-VEGF Injections, *n*	Retinal Lesion Size (mm^2)	Disease Duration (y, mo)
P01	Male	63, 7	nvAMD	OS	20	6	22.73	OD	29	8	18.95	2, 3
P02	Female	69, 0	nvAMD	OD	HM	0	20.23	OS	34	35	16.75	5, 7
P03	Female	83, 7	nvAMD	OS	HM	0	—	OD	29	31	16.31	6, 5
P04	Female	75, 10	nvAMD	OD	65	59	6.56	OS	68	17	1.87	5, 10
P05	Male	84, 4	nvAMD	OS	52	55	21.18	OD	67	0	32.29	5, 4
P06	Male	74, 3	nvAMD	OD	46	43	13.5	OS	75	8	11.73	13, 7
P07	Male	77, 5	nvAMD	OD	68	59	13.93	OD	71	1	20.92	6, 1
P08	Female	90, 10	nvAMD	OS	24	0	46.99	OD	31	51	27.6	13, 2
P09	Female	90, 4	nvAMD	OS	HM	3	50.97	OD	48	99	28.51	10, 3
P10	Male	75, 7	nvAMD	OD	85	84	13.59	OS	85	72	28.43	7, 8
P11	Male	87, 11	nvAMD	OS	50	16	8.72	OD	71	49	12.58	6, 6
P12	Male	76, 6	CSCR/nvAMD	OS	3	3	38.79	OD	42	3	19.02	8, 4
P13	Male	73, 2	nvAMD	OS	37	0	35.18	OD	48	15	37.47	11, 11
P14	Female	85, 1	nvAMD	OD	25	17	3.92	OS	68	23	5.41	9, 1

Disease duration refers to the point from bilateral onset. OD, oculus dexter (right eye); OS, oculus sinister (left eye); CSCR, central serous chorioretinopathy.

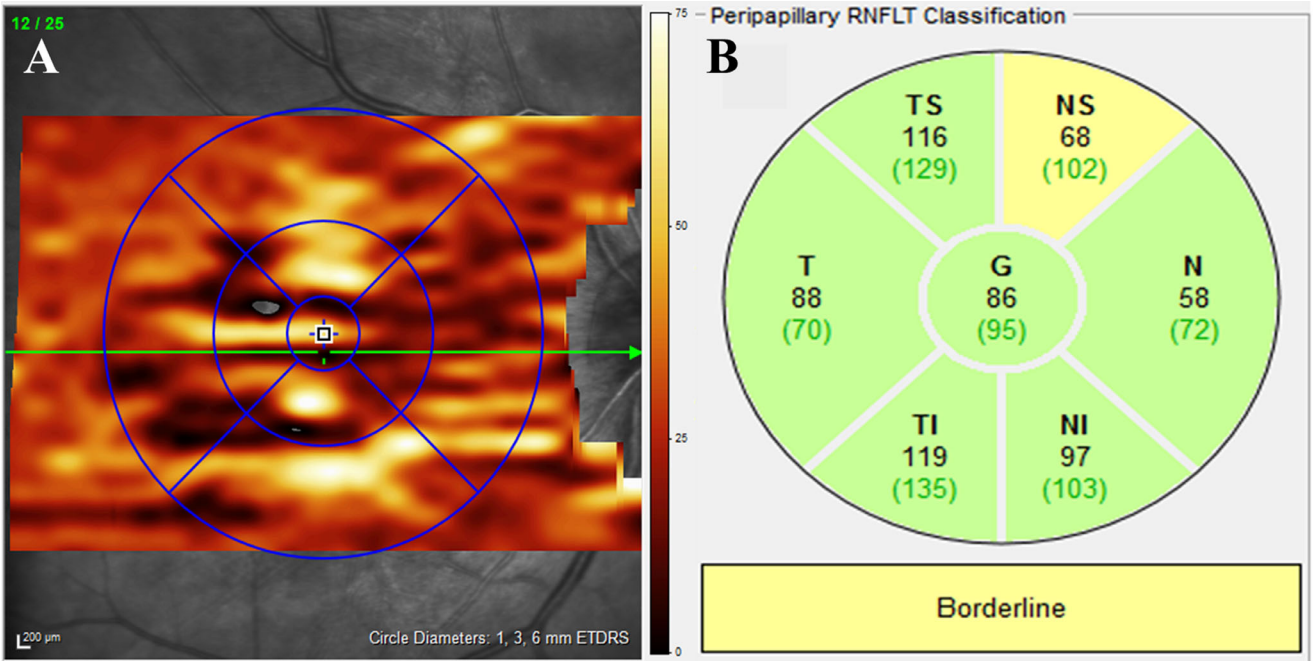

Figure 1. SD-OCT GCL and pRNFL classifications. (**A**) ETDRS diameter locations on the macular. GCL thickness was measured from the inner and middle rings representing the 1-mm- and 3-mm-diameter ETDRS locations referred to as the central macula (0°–5° eccentricity), with the outer ring representing the 6-mm-diameter ETDRS referred to as the peripheral macula (5°–10° eccentricity). The overlaid heatmap refers to the thickness of the GCL, with *darker colors* indicating regions of reduced thickness. The *horizontal green line* indicates the current slice of the B-scan also shown numerically in the *top left-hand corner* of the image. (**B**) pRNFL classification with the seven quadrants of the optic nerve head: NS, nasal superior; N, nasal; NI, nasal inferior; TI, temporal inferior; T, temporal; TS, temporal superior; G, global. Colors indicate quadrants in which values fall within normal limits (*green*) or are borderline (*yellow*); numbers shown in *green* inside the brackets represent normative values for those segments.

ipants is shown in Table 1, referring to the time at which the disease became bilateral. All participants had unilateral retinal disease prior to this time point; as a result, the effect of unilateral retinal disease on the following outcomes measures is unknown. Nevertheless, we would expect the most significant effect of retinal disease on the reported outcome measures to occur following bilateral vision loss.[1] Although participant P12 had an original diagnosis of central serous chorioretinopathy, at the point of recruitment to the study this participant had been re-diagnosed and was undergoing anti-VEGF treatment for bilateral nvAMD, hence their inclusion.

Thirty-three sighted controls were recruited from York Neuroimaging Centre between May 2018 and November 2019, completing the structural MRI procedures only. All participants were age-range matched (mean age, 71.02 years; age range, 65.01–83.03 years; 14 females) with normal or corrected-to-normal vision.

Design

In this cross-sectional design, routine clinical assessments took place no more than 2 weeks prior to the MRI assessments, detailed below.

Procedures

Anterior Visual Pathway. All participants completed structural assessments of each eye via SPECTRALIS SD-OCT (Heidelberg Engineering, Heidelberg, Germany) of the macula and optic nerve head, acquired through dilated pupils. Autoflourescence images of the central macular region were used to measure the extent of the scotoma in each eye for all participants, in terms of degrees of visual angle (Table 1). The border of the affected retina was traced using built-in software, with the resulting value showing the area of the affected region in square millimeters (Supplementary Fig. S1).

Best-Corrected Visual Acuity. Standard best-corrected visual acuity (BCVA) was measured in an illuminated room at 4 meters with the participant's spectacle correction in each eye using an Early Treatment Diabetic Retinopathy Study (ETDRS) letter chart. Participants P02, P03, and P09 were not able to read any letters in one eye and could only detect hand movements (HMs). For analysis purposes, the ETDRS letter score for that eye was set to 0 letters.

Macular GCL Thickness. Foveal volumetric scans acquired 25 frames in an area of 30° × 30° at 1536 × 1536 pixels. Infrared images of the macula enabled segmentation of the retinal layers using the built-in Heidelberg Eye Explorer software, version 1.9.17.0. Thickness measures were calculated for the GCL, with the central 1-mm- and 3-mm-diameter ETDRS locations representing the central macula (0°–5° eccentricity) and the 6-mm-diameter ETDRS location representing the peripheral macula (5°–10° eccentricity) (Fig. 1A).

pRNFL Thickness. The pRNFL thickness, acquired using a 3.5-mm-diameter disc (768 A-scans) centered over the optic disc, allowed for classification of seven quadrants of the optic nerve head: temporal, inferior temporal, superior temporal, nasal, inferior nasal, superior nasal, and global (all

quadrants). Built-in software analyzed all quadrants, identifying those that fell within or below normal thickness limits for the age range of each participant (Fig. 1B). It is important to note that the three nasal quadrants represent projections from the far peripheral retina, including retinal locations beyond that classified in the GCL assessment as the peripheral macula.

Analysis. One-sample *t*-tests established whether the BCVA for each eye was significantly different from normal, determined as an ETDRS letter score of 84 which is equivalent to 6/6 Snellen acuity or 0 logMAR. Normative mean GCL thickness values were extracted from a different study using the same model of SD-OCT machine.[15] Normative means were extracted from a group of age-range-matched control subjects, ranging between 69 and 87 years. Normative pRNFL thickness values were taken from the SD-OCT output of the current study. BCVA acquired on the same day was used to determine the better and worse seeing eye for all participants (Table 1). Paired-samples *t*-tests then established whether the two eyes were significantly different from the normative means for the two clinical measures.

Pearson correlations were carried out between BCVA and retinal lesion size and between total macular GCL thickness, global pRNFL thickness, and the number of anti-VEGF injections that the worse and better seeing eyes received, investigating the possible relationship between increased anti-VEGF injections and reduced retinal structure.

Posterior Visual Pathway. MRI assessments were completed no more than 2 weeks following the clinical assessments. MRI took place on a 3-tesla MRI scanner (MAGNETOM Prisma; Siemens Healthcare GmbH, Erlangen, Germany) using a 64-channel head receiver array coil. All participants were instructed to lie as still as possible during the scan. Foam padding was used around the head to minimize movement, and earplugs were provided to protect against scanner noise. Two isotropic T1-weighted magnetization-prepared rapid gradient-echo (T1w MP-RAGE; repetition time [TR] = 2400 ms, echo time [TE] = 2.28 ms, inversion time [TI] = 1010 ms, flip angle = 8°, voxel size = 0.8 × 0.8 × 0.8 mm, matrix size = 256 × 256 × 167 mm) and two isotropic T2-weighted sampling perfection with application-optimized contrast using different flip angle evolutions (T2w SPACE; TR = 3200 ms, TE = 563 ms, voxel size = 0.8 × 0.8 × 0.8 mm, matrix size = 256 × 256 × 167 mm) anatomical volumes were acquired following guidelines from the Human Connectome Project.[16]

Analysis. Cortical reconstruction and volumetric segmentation were performed using the Human Connectome Project analysis pipeline (version 6.0), incorporating the Freesurfer analysis suite (version 6.0). The three-stage structural analysis pipeline includes alignment of T1w and T2w images, bias field correction, volume segmentation, reconstruction of white and pial surfaces, and surface registration.[16] Two structural characteristics of the cerebral cortex (gray matter) were assessed: cortical volume of the entire occipital cortex and mean cortical thickness of the occipital pole and calcarine sulcus (see Fig. 5A) following the same rationale described in our previous study.[1] Mean gray matter volume was extracted from each parcellation within the occipital cortex region of interest (ROI), from both the left and right hemispheres. A hemisphere average was then calculated for each participant to create the final entire occipital cortex ROI. A one-way analysis of covariance (ANCOVA) assessed changes in cortical volume between the controls and central vision loss group, controlling for whole-brain volume. Mean cortical thickness was extracted following this same procedure for two regions representing the central (occipital pole) and peripheral (calcarine sulcus) retina. A one-way ANOVA compared mean cortical thickness within each ROI between the controls and central vision loss group.

Exploratory Relationship Between Measures. The second aim of the study was to explore the potential relationship between changes observed in the anterior and posterior visual pathways, specifically addressing the following questions:

1. *Can changes in retinal structure predict changes in cortical structure?* The first Pearson correlation assessed whether changes to GCL and pRNFL thickness are significant predictors of reduced volume of the entire occipital cortex. The second set of Pearson correlations assessed whether changes in central macular GCL thickness, peripheral macular GCL thickness, and temporal pRNFL thickness were significant predictors of reduced cortical thickness in the occipital pole, representing the central retina. The third correlation assessed whether changes in nasal pRNFL thickness were a significant predictor of reduced cortical thickness in the calcarine sulcus, representing the peripheral retina.
2. *Can changes in cortical structure predict changes in visual function?* Two Pearson correlations were conducted to establish whether changes in cortical thickness in the occipital pole (cortical representation of the central macula) or the calcarine sulcus (cortical representation of the peripheral macula) can predict visual function (BCVA).
3. *Can disease characteristics such as bilateral disease duration and number of anti-VEGF treatments predict retinal structure, visual function, or cortical structure?* Pearson correlations were conducted between bilateral disease duration and total macular GCL thickness and global pRNFL thickness (retinal structure), BCVA (visual function), and cortical volume and thickness (cortical structure).

Results

Anterior Visual Pathway

Although data from all participants were included in the BCVA analysis, participant P01 was excluded from the GCL and pRNFL thickness analyses due to segmentation issues (see Supplementary Fig. S2) and data exceeding 2 SD from the mean.

BCVA. One-sample *t*-tests revealed that BCVA values for both eyes were significantly reduced from normal: worse eye, $t(13) = -6.670$, $P = 0.000015$, 2-tailed; better eye, $t(13) = -5.628$, $P = 0.000082$, 2-tailed (Fig. 2). Assessing whether BCVA is correlated with the size of the retinal lesion, despite a small effect size in the worse seeing eye ($R^2 = -0.150$), Pearson correlations revealed a non-significant relationship in both the worse eye ($R = -0.387$, $P = 0.172$) and the better seeing eye ($R = -0.176$, $P = 0.546$) (Fig. 2; see Table 3).

Macular GCL Thickness. Total macular GCL thickness (the average of all three macular locations: 1-mm-, 3-mm-, and 6-mm-diameter ETDRS) was greater in the worse compared to the better seeing eye, although this was not significant, $t(11) = 0.689$, $P = 0.505$ (Table 2). Compared

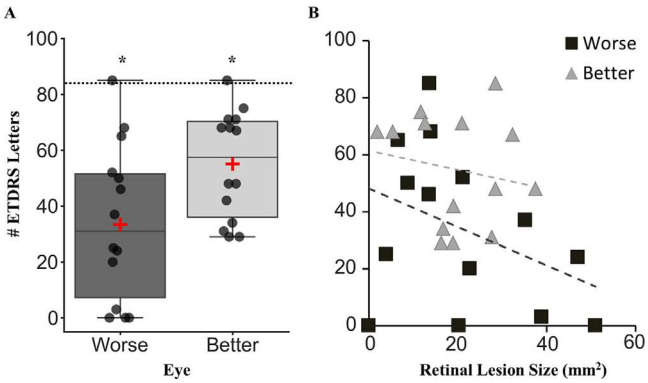

Figure 2. Box plot showing the BCVA presented as the number of ETDRS letters for all patients (**A**), with a scatterplot showing the non-significant Pearson correlation between BCVA and retinal lesion size (**B**) for the worse (*dark gray*) and better (*light gray*) seeing eye. In (**A**), the *horizontal lines* represent the median with upper and lower whiskers representing scores outside the middle 50%. *Red crosses* indicate the mean BCVA values. *Dots* represent data from each participant. The *horizontal dashed line* represents normal ETDRS of 84 letters, equivalent to 6/6 Snellen acuity and 0.0 logMAR. *Significant at $P = 0.001$, 2-tailed. In (**B**), each shape represents data from an individual participant, and the *dashed lines* represent the lines of best fit.

Table 2. Mean and SEM for the Worse and Better Seeing Eye Across the Assessments in the Anterior Visual Pathway

	Normative	Worse Seeing Eye		Better Seeing Eye	
	Mean	Mean	SEM	Mean	SEM
BCVA (no. of ETDRS letters)	84	**33.9**	7.5	**54.7**	5.2
GCL thickness (µm)					
Total macula	36.8	**26.2**	2.0	**24.3**	2.5
Central macula	40.2	**26.4**	2.8	**23.6**	3.1
Peripheral macula	32.5	**25.6**	1.3	**25.6**	1.9
pRNFL thickness (µm)					
Global	95	**82.8**	3.8	**86.2**	3.8
Inferior temporal	135	**99.5**	6.4	**111.8**	6.2
Temporal	72	60.8	8.4	68.5	3.4
Superior temporal	130	122.3	6.6	117.0	7.2
Inferior nasal	103	97.2	7.7	100.9	8.2
Nasal	72	66.8	3.0	63.9	4.8
Superior nasal	102	90.5	7.8	94.0	5.7

Bold values indicate those that are significantly different from the normative mean. SEM, standard error of the mean.

against the normative mean of 36.8 µm, both the worse seeing eye, $t(11) = -5.257$, $P = 0.000269$, 2-tailed, and the better seeing eye, $t(12) = -4.977$, $P = 0.000321$, 2-tailed, were significantly thinner (Fig. 3A).

Central macular GCL thickness (the average of the 1-mm- and 3-mm-diameter ETDRS locations; 0°–5° eccentricity) was greater in the worse compared to the better seeing eye, although this was not significant, $t(11) = 0.780$, $P = 0.452$ (Table 2). Compared against the normative mean of 40.2 µm, both the worse seeing eye, $t(11) = -4.895$, $P = 0.000475$, 2-tailed, and the better seeing eye, $t(12) = -5.409$, $P = 0.000158$, 2-tailed, were significantly thinner (Fig. 3B).

Peripheral macular GCL thickness values (measured as the 6-mm-diameter ETDRS location; 5°–10° eccentricity) were not significantly different between eyes, $t(11) = 0.038$, $P = 0.970$ (Table 2). When compared against the normative mean of 32.5 µm, both the worse seeing eye, $t(11) = -5.262$, $P = 0.000268$, 2-tailed, and the better seeing eye, $t(12) = -3.728$, $P = 0.003$, 2-tailed, were significantly thinner (Fig. 3C).

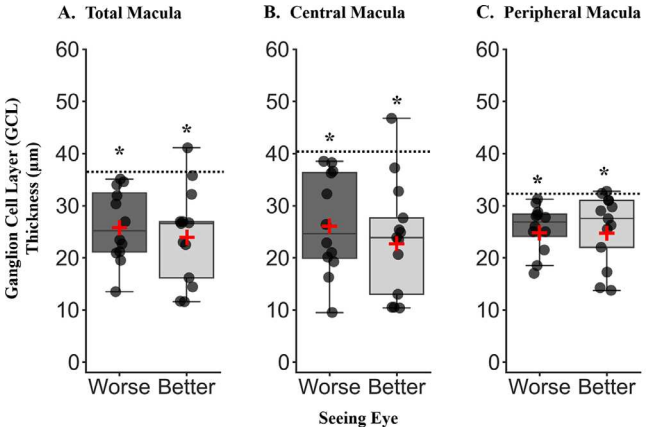

Figure 3. Macula ganglion cell layer (GCL) thickness for the worse and better seeing eye by ETDRS location. (**A**) Total macula GCL thickness, averaged across the 1-mm-, 3-mm-, and 6-mm-diameter ETDRS locations. (**B**) Central macula GCL thickness calculated as an average of the 1-mm- and 3-mm-diameter ETDRS locations. (**C**) Peripheral macula GCL thickness representing the 6-mm-diameter ETDRS location. For all box plots, *horizontal lines* represent the median, and *upper* and *lower whiskers* represent scores outside the middle 50%. *Red crosses* indicate the mean thickness value. *Dots* represent data from each participant. *Horizontal dashed lines* represent the normative mean taken from age-range-matched sighted controls.[15] *Significantly different from normative means at $P < 0.001$, 2-tailed.

pRNFL Thickness. Mean global pRNFL thickness was calculated as the average across all six quadrants shown in Figure 4. Thickness values were not significantly reduced in the worse compared to the better seeing eye, $t(11) = -0.481$, $P = 0.640$ (Table 2); however, both eyes were significantly thinner than the normative mean of 95.0 µm: worse eye, $t(11) = -3.229$, $P = 0.008$; better eye, $t(12) = -2.357$, $P = 0.036$. pRNFL thickness in the temporal quadrants, representing projections from the central retina (Fig. 4), were not significantly different between eyes for the superior temporal quadrant, $t(11) = 0.824$, $P = 0.428$; temporal quadrant, $t(11) = -1.173$, $P = 0.266$; and inferior temporal quadrant, $t(11) = -1.187$, $P = 0.260$ (Table 2). Compared against the normative mean values in each quadrant, both eyes were significantly thinner for the inferior temporal quadrant (normative mean [NM] = 135.0 µm): worse eye, $t(11) = -5.531$, $P = 0.000178$; better eye, $t(12) = -3.716$, $P = 0.003$. However, there was no significant difference between either eye and the normative mean in the temporal quadrant (NM = 72.0 µm): worse eye, $t(11) = -1.337$, $P = 0.208$; better eye, $t(12) = -1.005$, $P = 0.335$. Also, there was not a significant difference in the superior temporal quadrant (NM = 130.0 µm): worse eye, $t(11) = -1.183$, $P = 0.262$; better eye, $t(12) = -1.814$, $P = 0.095$.

pRNFL thickness across the nasal quadrants, representing projections from the far peripheral retina (beyond the 10° visual angle captured by the GCL analyses above) were measured to investigate whether loss in peripheral retinal projections might explain the significant atrophy of the cortical representation of the peripheral retina, the calcarine sulcus (Fig. 4). There was no significant difference in mean

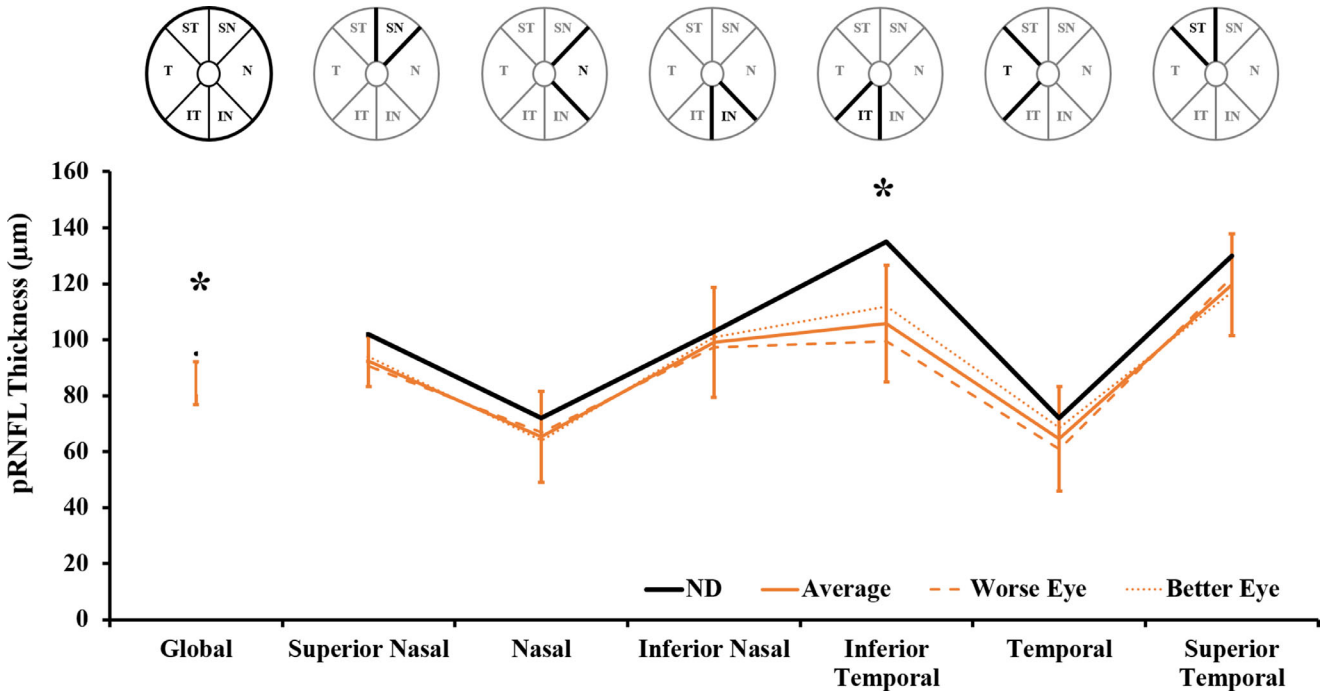

Figure 4. pRNFL thickness of the optic nerve head stratified by quadrant for the central vision loss group. Schematics above the line graph denote the quadrant of interest for each dataset. The *dashed line* represents thickness values from each quadrant for the worse seeing eye, and the *dotted line* represents the better seeing eye. An average of the two eyes is shown by the *full orange line*; the *error bars* represent the standard error of the mean. The *black line* represents normative mean values built into the SPECTRALIS SD-OCT machine. Global thickness is calculated as the average of all nasal and temporal quadrants. *Significantly different from normative mean at $P < 0.001$, 2-tailed.

thickness between eyes in the nasal quadrant, $t(11) = 1.004$, $P = 0.337$; the superior nasal quadrant, $t(11) = -0.310$, $P = 0.762$; and inferior nasal quadrant, $t(11) = -0.230$, $P = 0.822$ (Table 2). Compared against the normative mean values in each quadrant, thickness values were not significantly different for either eye in the inferior nasal quadrant (NM = 103.0 µm): worse eye, $t(11) = -0.757$, $P = 0.465$; better eye, $t(12) = -0.252$, $P = 0.805$; the nasal quadrant (NM = 72.0 µm): worse eye, $t(11) = -1.772$, $P = 0.104$; better eye, $t(12) = -1.675$, $P = 0.120$; nor the superior nasal quadrant (NM = 102.0 µm): worse eye, $t(11) = -1.475$, $P = 0.168$; better eye, $t(12) = -1.409$, $P = 0.184$.

Anti-VEGF Injections. Pearson correlations revealed there was no significant relationship between the number of anti-VEGF injections received in either the worse or better seeing eye and total macular GCL or global pRNFL thickness (Table 3).

Posterior Visual Pathway

Cortical Volume. Despite a medium effect size, there was a non-significant reduction in cortical volume of the occipital lobes in the patient group compared to sighted controls after controlling for whole brain volume: $F(1,44) = 3.339$, $P = 0.074$, $\eta_p^2 = 0.071$ (Fig. 5B).

Cortical Thickness. Significant cortical atrophy was found via a reduction in cortical thickness in the retinotopic representation of the central (diseased) retina—namely, the occipital pole, with a large effect size: $F(1,46) = 13.086$, $P = 0.001$, $\eta^2 = 0.225$). Surprisingly, significant cortical atrophy was also observed with a reduction in cortical thickness in the retinotopic representation of the peripheral retina—namely, the calcarine sulcus, also with a large effect size: $F(1,46) = 12.122$, $P = 0.001$, $\eta^2 = 0.212$ (Fig. 5C).

Exploratory Relationship Between Measures

The following correlations were all Bonferroni corrected according to the number of correlations performed within each of the exploratory analyses described in the methods.

Can Changes in Retinal Structure Predict Changes in Cortical Structure? Pearson correlations between changes to the anterior and posterior visual pathways were non-significant, but they identified two relationships for further investigation due to the small effect sizes found: cortical volume and total GCL ($R^2 = 0.105$) and global pRNFL ($R^2 = 0.202$) thickness (Table 3).

Can Changes in Cortical Structure Predict Changes in Visual Function? Pearson correlations between cortical thickness in the occipital pole and calcarine sulcus were not significantly correlated with BCVA in either the worse or better seeing eye (Table 3). However, there was a medium effect size ($R^2 = 0.331$, $P = 0.062$) and a small effect size ($R^2 = 0.263$, $P = 0.122$) when correlating cortical thickness in the occipital pole and BCVA in the worse and better seeing eyes, respectively. The effect sizes observed here suggest that further investigation of these relationships is required in larger patient cohorts to establish whether they reach significance.

Can Disease Characteristics Such As Bilateral Disease Duration and Number of Anti-VEGF Treatments Predict Retinal Structure, Visual Function, or Cortical Structure? There was a large effect size observed correlating bilateral disease duration and total macular GCL thickness in the better seeing eye ($R^2 = -0.646$, $P = 0.002$), suggesting that

Table 3. Pearson Correlation, Effect Size, Significance, and Bonferroni-Corrected Significance Values Assessing Exploratory Associations Among Disease Characteristics in the Anterior and Posterior Visual Pathway

	Worse Seeing Eye				Better Seeing Eye			
	R	***R*²**	***P***	**BCp**	***R***	***R*²**	***P***	**BCp**
BCVA vs. retinal lesion size	−0.387	−0.150	0.172	0.172	−0.176	−0.031	0.546	0.546
Can changes in retinal structure predict changes in cortical structure?								
Total macular GCL thickness vs. cortical volume ($n = 13$)	0.324	0.105	0.304	0.608	0.003	0.000	0.992	0.999
Global pRNFL thickness vs. cortical volume ($n = 13$)	0.148	0.022	0.647	0.999	0.450	0.202	0.123	0.246
Central macular GCL thickness vs. mean cortical thickness OP ($n = 13$)	−0.134	−0.018	0.677	0.999	0.274	0.075	0.364	0.999
Peripheral macular GCL thickness vs. mean cortical thickness OP ($n = 13$)	−0.141	−0.019	0.663	0.999	−0.059	−0.003	0.847	0.999
Average temporal pRNFL thickness vs. mean cortical thickness OP ($n = 13$)	0.049	0.002	0.880	0.999	−0.135	−0.018	0.660	0.999
Average nasal pRNFL thickness vs. mean cortical thickness CS ($n = 13$)	−0.165	−0.027	0.609	0.609	0.202	0.041	0.509	0.509
Can changes in cortical structure predict changes in visual function?								
Mean cortical thickness OP vs. BCVA ($n = 14$)	0.576	0.331	0.031	0.062	0.513	0.263	0.061	0.122
Mean cortical thickness CS vs. BCVA ($n = 14$)	0.332	0.110	0.246	0.492	0.142	0.020	0.629	0.999
Can disease characteristics such as bilateral disease duration and number of anti-VEGF treatments predict retinal structure, visual function, or cortical structure?								
Bilateral disease duration vs.								
Total macular GCL thickness ($n = 13$)	−0.140	−0.019	0.665	0.999	**−0.804***	**−0.646**	**0.001**	**0.002**
Global pRNFL thickness ($n = 13$)	0.367	0.135	0.240	0.480	0.003	0.000	0.992	0.999
BCVA ($n = 14$)	−0.083	−0.007	0.777	0.777	0.073	0.005	0.805	0.805
Cortical volume ($n = 14$)	−0.168	−0.028	0.566	0.999	—	—	—	—
Mean cortical thickness OP ($n = 14$)	0.223	0.049	0.444	0.999	—	—	—	—
Mean cortical thickness CS ($n = 14$)	−0.027	−0.000	0.927	0.999	—	—	—	—
Number of anti-VEGF injections vs.								
Total macular GCL thickness ($n = 13$)	−0.266	−0.071	0.403	0.806	−0.084	−0.007	0.785	0.999
Global pRNFL thickness ($n = 13$)	0.036	0.001	0.913	0.999	−0.195	−0.038	0.524	0.999

* Bonferroni corrected at $P = 0.025$.

BCp, Bonferroni-corrected *P*; OP, occipital pole; CS, calcarine sulcus.

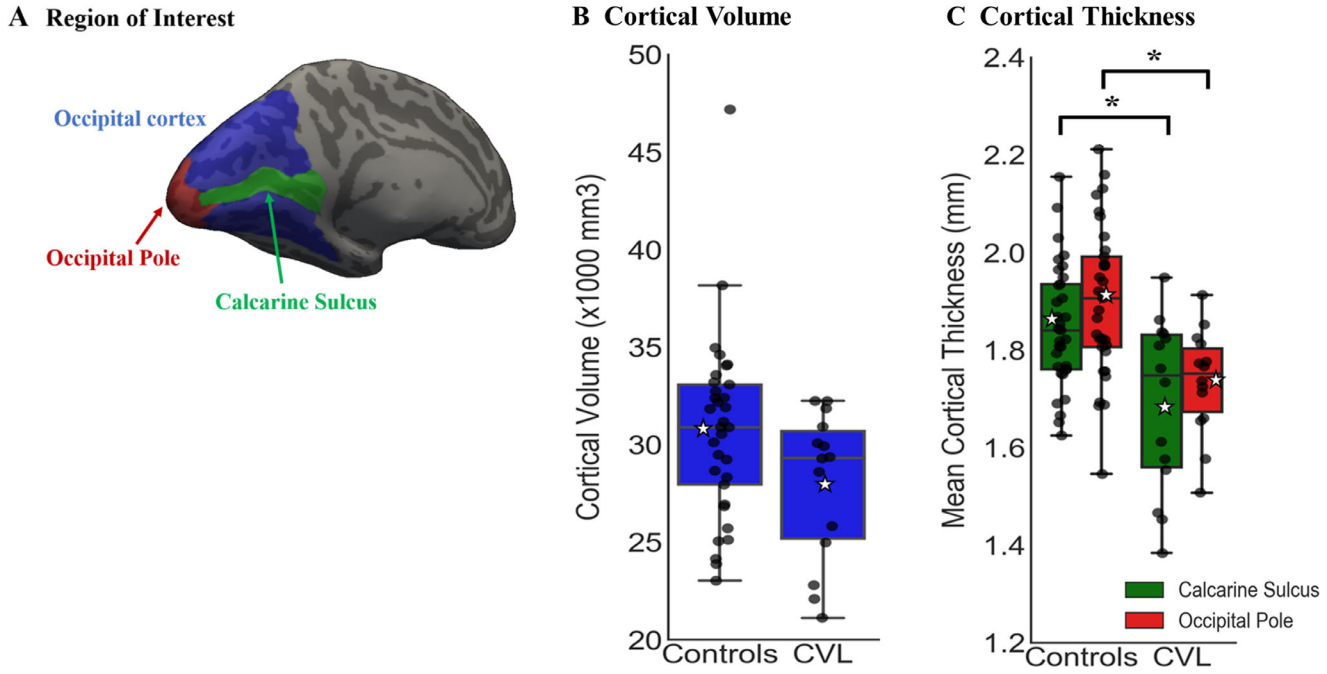

Figure 5. Structural MRI ROI. (**A**) Inflated medial surface of the left hemisphere showing the three ROIs. The entire visual cortex is represented by the regions shown in *blue*, including the cortical representations of the central visual field, the occipital pole (shown in *red*), and the peripheral visual field, the calcarine sulcus (shown in *green*). Box plots show the cortical volume of the entire occipital cortex (**B**) and mean cortical thickness (**C**) for the sighted controls and central vision loss (CVL) participants. The *horizontal lines* represent the median, and the upper and lower whiskers represent scores outside the middle 50%. *White stars* represent the mean. Data for each individual participant are overlaid on the box plots and shown as *black dots*. *$P = 0.001$.

the longer the disease duration, the thinner the GCL. A small effect size was also found when correlating bilateral disease duration with global pRNFL thickness ($R^2 = 0.135$), which would warrant further investigation in a larger cohort to confirm significance.

Discussion

This study highlights structural changes occurring in the anterior and posterior visual pathways in patients with long-term central retinal disease, reporting significant relationships between structural changes, disease characteristics, and visual function. We found that longer bilateral disease duration significantly predicted reduced macular GCL thickness, and reduced cortical thickness of the occipital pole significantly predicted reduced visual acuity. To the best of our knowledge, this is the first time a correlation between cortical structure and visual function in long-term acquired central retinal disease has been reported.

Supporting previous research, assessments of the anterior visual pathway (eye) reveal significant thinning to the GCL in both the better and worse seeing eyes and at all macular ETDRS locations in central retinal disease.[4,6,17,18] We also report significant reductions in global pRNFL thickness compared to normative data, with specific thinning in the inferior temporal quadrant, consistent with previous research.[12] Together, these results suggest that transneuronal degeneration of the GCL may be occurring following long-term reduced input from the photoreceptors. It may well be that changes in GCL thickness are a more sensitive biomarker of disease progression in diseases including nvAMD, in which macular edemas are common, compared with assessing total macular thickness alone. Changes to the structure of the central macula may also lead to changes in the thickness of projections to the optic nerve head, indicating a progressive loss of neurons in both outer and inner retinal layers.

The observed retinal thinning could possibly be explained by the advancing disease affecting the inner retinal layer and in turn the pRNFL; however, our results indicate that only thinning of the macular GCL could be predicted by increasing disease duration. This supports previous literature showing that retinal remodeling occurs in nvAMD and that inner retinal layers, including the GCL, become affected as nvAMD progresses.[4–6] There is also debate whether repeated anti-VEGF injections accelerate atrophy of intraocular tissues.[5,17–19] Among the 14 patients included in this current study, an average of 54.1 anti-VEGF injections were received (worse eye, 24.6; better eye, 29.4) over an average 7 years, 9 months, which is greater than previously reported.[5,17,18] However, we did not find any significant relationship between the number of injections received and reduced GCL or pRNFL thickness.

The next element of the current study quantified changes to the posterior visual pathway (brain) associated with central retinal disease. Supporting previous research, we found significant evidence of cortical atrophy associated with long-term central retinal disease with reduced cortical thickness in the occipital pole, the cortical representation of the affected central retina.[1,10,11,13,14] Surprisingly, we also report significant cortical atrophy of the calcarine sulcus, the cortical representation of the peripheral retina, which should be largely unaffected in nvAMD. In our previous study, we reported cortical thinning in the occipital pole but not calcarine sulcus in a cohort with bilateral central retinal disease after 3 to 6 years,[1] whereas most participants in

the current study had had bilateral disease for considerably longer (Table 1). This possibly indicates that, as the retinal disease has advanced in this cohort to occupy more peripheral retinal locations, the loss of visual input cascades down the visual pathway and is measurable in the cortex.

In light of these reported changes, the final element of this study aimed to explore whether changes to the anterior and posterior visual pathways may be related to each other or to other variables. Progression of central retinal disease due to nvAMD moves from the photoreceptor layer to more inner retinal layers including the GCL, which in turn projects to the visual cortex via the optic radiations. Investigating the relationship between the two components of the visual pathway addressed whether neuronal loss in one pathway can lead to neuronal loss in the other. We did not find a direct relationship between the extent of structural changes in the anterior and posterior pathways. However, a small effect size was observed in positive correlations between cortical volume and both total GCL and global pRNFL thickness. This observation warrants further investigation in a larger patient cohort to establish if the correlation is significant, suggesting that either the two are uncoupled and occur independently of one another or the loss of visual input to the anterior visual pathway alone may be sufficient to lead to cortical atrophy in the posterior visual pathway.

Supporting the latter hypothesis, although we did not find a direct relationship between cortical structure and visual performance, we did reveal a positive correlation with a medium effect size between decreased cortical thickness in the occipital pole and reduced BCVA in the better seeing eye. Existing knowledge suggests that maintained structure of the central macula is essential to see in fine detail, including BCVA.[20] Importantly, however, this current study may suggest that BCVA also relies on maintained structure of the visual cortex, specifically the occipital pole. Reduced BCVA may in fact be due to both retinal and cortical loss. Although changes in brain morphology have been linked with reduced visual acuity previously in albinism,[21] to the best of our knowledge this is the first study to suggest that BCVA may be related to reduced cortical thickness in the occipital pole in long-term acquired central retinal disease, a finding that warrants further investigation in a larger cohort to establish significance.

In conclusion, this study demonstrates that in long-term central retinal disease there are significant structural changes to both the anterior and posterior visual pathways. Changes to the anterior visual pathway suggest possible retinal remodeling and transsynaptic degeneration. Thus, monitoring GCL thickness in individuals without active edemas may provide a sensitive biomarker of nvAMD disease progression. Changes to the posterior visual pathway reveal significant cortical atrophy in not only the central retinal representation receiving input from affected macula but also the peripheral retinal representation. Moreover, cortical thinning of the central retinal representation may correlate with reduced BCVA. This, combined with longitudinal data from our previous study,[1] suggests that earlier intervention to prevent vision loss may prevent further cortical changes, which in turn may affect visual function.

However, the presence or absence of correlations between measures does not necessarily allow us to infer causation or the order in which changes occur. For example, do reductions in retinal thickness result in impaired BCVA, which then results in cortical atrophy, or is impaired BCVA alone sufficient to cause cortical atrophy and together these result in reduced retinal thickness? These questions may be addressed better by longitudinal studies following multiple anterior and posterior measures in the same clinical cohort.

It is also important to note here that the relatively small sample size in this study is a weakness that may limit the statistical power to detect some effects. We feel there are intriguing relationships to be examined further based on effect sizes outlined in this study, and investigations in larger cohorts of patients would be warranted in the future.

Overall, this information is important to future research into patient selection for vision restoration techniques. The ability to measure the impact of long-term vision loss on the extent of cortical atrophy of the posterior visual pathway is vital, as the success of such restorative devices relies on the posterior visual pathway remaining viable to restored visual input.

Acknowledgments

The authors thank with thanks the ESRC +3 White Rose Doctoral Training Centre scholarship (ES/J500215/1), the research and development team, and the ophthalmology research team at York and Scarborough Teaching Hospitals NHS Foundation Trust.

Disclosure: **R.L.W. Hanson**, None; **H.A. Baseler**, None; **A. Airody**, None; **A.B. Morland**, None; **R.P. Gale**, None

References

1. Hanson RLW, Gale RP, Gouws AD, et al. Following the status of visual cortex over time in patients with macular degeneration reveals atrophy of visually deprived brain regions. *Invest Ophthalmol Vis Sci*. 2019;60(15):5045–5051.
2. Nixon DR, Flinn AP. Evaluation of contrast sensitivity and other visual function outcomes in neovascular age-related macular degeneration patients after treatment switch to aflibercept from ranibizumab. *Clin Ophthalmol*. 2017;11:715–721.
3. Airody A, Venugopal D, Allgar V, Gale RP. Clinical characteristics and outcomes after 5 years pro re nata treatment of neovascular age-related macular degeneration with ranibizumab. *Acta Ophthalmol*. 2015;93(6):e511–e512.
4. Zucchiatti I, Parodi MB, Pierro L, et al. Macular ganglion cell complex and retinal nerve fiber layer comparison in different stages of age-related macular degeneration. *Am J Ophthalmol*. 2015;160(3):602–607.e1.
5. Martínez-de-la-Casa JM, Ruiz-Calvo A, Saenz-Frances F, et al. Retinal nerve fiber layer thickness changes in patients with age-related macular degeneration treated with intravitreal ranibizumab. *Invest Ophthalmol Vis Sci*. 2012;53(10):6214–6218.
6. Beck M, Munk MR, Ebneter A, Wolf S, Zinkernagel MS. Retinal ganglion cell layer change in patients treated with anti-vascular endothelial growth factor for neovascular age-related macular degeneration. *Am J Ophthalmol*. 2016;167:10–17.
7. Fitzgibbon T, Taylor SF. Retinotopy of the human retinal nerve fibre layer and optic nerve head. *J Comp Neurol*. 1996;375(2):238–251.
8. Jansonius NM, Nevalainen J, Selig B, et al. A mathematical description of nerve fiber bundle trajectories and their variability in the human retina. *Vision Res*. 2009;49(17):2157–2163.
9. Lee EK, Yu HG. Ganglion cell-inner plexiform layer and peripapillary retinal nerve fiber layer thicknesses in age-related macular degeneration. *Invest Ophthalmol Vis Sci*. 2015;56(6):3976–3983.

10. Boucard CC, Hernowo AT, Maguire RP, et al. Changes in cortical grey matter density associated with long-standing retinal visual field defects. *Brain*. 2009;132(pt 7):1898–1906.
11. Hernowo AT, Prins D, Baseler HA, et al. Morphometric analyses of the visual pathways in macular degeneration. *Cortex*. 2014;56:99–110.
12. Malania M, Konra J, Jägle H, Werner JS, Greenlee MW. Compromised integrity of central visual pathways in patients with macular degeneration. *Invest Ophthalmol Vis Sci*. 2017;58(7):2939–2947.
13. Plank T, Frolo J, Brandl-Rühle S, et al. Gray matter alterations in visual cortex of patients with loss of central vision due to hereditary retinal dystrophies. *NeuroImage*. 2011;56(3):1556–1565.
14. Prins D, Plank T, Baseler HA, et al. Surface-based analyses of anatomical properties of the visual cortex in macular degeneration. *PLoS One*. 2016;11(1):e0146684.
15. Nieves-Moreno M, Martínez-de-la-Casa JM, Cifuentes-Canorea P, et al. Normative database for separate inner retinal layers thickness using spectral domain optical coherence tomography in Caucasian population. *PLoS One*. 2017;12(7):e0180450.
16. Glasser MF, Sotiropoulos SN, Wilson JA, et al. The minimal preprocessing pipelines for the Human Connectome Project. *NeuroImage*. 2013;80:105–124.
17. Lee SW, Sim HA, Park JY, et al. Changes in inner retinal layer thickness in patients with exudative age-related macular degeneration during treatment with anti-vascular endothelial growth factor. *Medicine (Baltimore)*. 2020;99(17):e19955.
18. Aşikgarip N, Temel E, Örnek K. Macular ganglion cell complex changes in eyes treated with aflibercept for neovascular age-related macular degeneration. *Photodiagnosis Photodyn Ther*. 2021;35:102383.
19. Horsley MB, Mandava N, Maycotte MA, Kahook MY. Retinal nerve fiber layer thickness in patients receiving chronic anti-vascular endothelial growth factor therapy. *Am J Ophthalmol*. 2010;150(4):558–561.
20. Lim LS, Mitchell P, Seddon JM, Holz FG, Wong TY. Age-related macular degeneration. *Lancet*. 2012;379(9827):1728–1738.
21. Bridge H, von dem Hagen EAH, Davies G, et al. Changes in brain morphology in albinism reflect reduced visual acuity. *Cortex*. 2014;56:64–72.

Investigative Ophthalmology & Visual Science